International Journal of Solids and Structures 47 (2010) 58–70

Contents lists available at ScienceDirect

International Journal of Solids and Structures

journal homepage: www.elsevier.com/locate/ijsolstr

Representations of elastic fields of circular dislocation and disclination loops in terms of spherical harmonics and their application to various problems of the theory of defects

Anna L. Kolesnikova [a], Alexey E. Romanov [b,c,*]

[a] Institute of Problems of Mechanical Engineering, RAS, St. Petersburg 199178, Russia
[b] Ioffe Physical Technical Institute, RAS, St. Petersburg 194021, Russia
[c] Polytechnique School, Aristotle University of Thessaloniki, Thessaloniki 54124, Greece

ARTICLE INFO

Article history:
Received 13 May 2009
Received in revised form 20 August 2009
Available online 15 September 2009

Keywords:
Circular twist disclination loop
Circular prismatic dislocation loop
Elasticity
Spherical harmonics
Boundary-value problems

ABSTRACT

Elastic fields of circular dislocation and disclination loops are represented in explicit form in terms of spherical harmonics, i.e. via series with Legendre and associated Legendre polynomials. Representations are obtained by expanding Lipschitz-Hankel integrals with two Bessel functions into Legendre series. Found representations are then applied to the solutions of elasticity boundary-value problems of the theory of defects and to the calculation of elastic fields of segmented spherical inclusions. In the framework of virtual circular dislocation–disclination loops technique, a general scheme to solving axisymmetric elasticity problems with boundary conditions specified on a sphere is given. New solutions for elastic fields of a twist disclination loop in a spherical particle and near a spherical pore are demonstrated. The easy and straightforward way for calculations of elastic fields of segmented spherical inclusion with uniaxial eigenstrain is shown.

1. Introduction

Loop configurations of dislocation and disclination defects are routinely used in the analysis of physical and mechanical behavior of various materials. This is caused by the facts of experimental observation of defect loops and exploring loop properties in the modeling of materials behavior. Glide and prismatic dislocation loops are formed in crystalline materials in the course of plastic deformation (Hirth and Lothe, 1982), thermal or radiation treatment (Was, 2007), whereas twist disclination loops are typical for polymers (Li and Gilman, 1970). Mesoscopic disclination (Romanov and Vladimirov, 1992) and general Somigliana dislocation (Asaro, 1975) loops were used in representing ensembles of lattice defects in deformed materials. Physical models describing the behavior of defect loops are essentially based on the calculation and the analysis of their elastic fields: displacements, strains and stresses. On the other hand, elastic fields of loop defects can be considered as elementary blocks for construction of the solutions for more involved elasticity problems, e.g. for cracks (Hills et al., 1996), inclusions (Mura, 1987), and elasticity boundary-value problems (Kolesnikova and Romanov, 2004). Present work is devoted to the finding of new representations for elastic fields of circular dislocation and disclination loops involving spherical harmonic functions, i.e. Legendre polynomials.

Among possible studied defect loop shapes circular loops were treated in greatest detail. Below we overview only the results obtained for elastically isotropic solids. Starting from the work by Kröner (1958), where his own results together with early results by Pfleiderer and Keller, were given, the elastic fields and energies of circular prismatic and glide (shear) dislocation loops in infinite elastic media were studied by Kroupa (1960, 1962), Bullough and Newman (1960), De Wit (1960), Owen and Mura (1967), Marcikowski and Sree Harsha (1968), Bushueva et al. (1974), and Povstenko (1995). More recently (Khraishi et al., 2000a,b), delivered a closed form analytical solutions for stresses and displacements of general translational circular Volterra dislocation loops that are characterized by an arbitrary Burgers vector. For disclination (rotation Volterra dislocation, which is characterized by an axial vector of rotation, i.e. Frank vector) loops the first solution was published by Owen and Mura (1967), in case of a rotational dislocation, that later was called "circular edge disclination" (Huang and Mura, 1970) and finally accepted the name "twist disclination loop". More solutions for twist and wedge disclination loops in infinite isotropic elastic media were given by Liu and Li (1971), Kuo and Mura (1972a), Kuo et al. (1973), and Povstenko and Matkovski (2000). Interesting connection of the twist disclination loop solution with the problem of a shrink-fit shaft subjected to torsion can be found in the results reported by Sackfield et al. (2002).

* Corresponding author. Address: Ioffe Physical Technical Institute, RAS, St. Petersburg 194021, Russia.
E-mail address: aer@mail.ioffe.ru (A.E. Romanov).

0020-7683/$ - see front matter © 2009 Elsevier Ltd. All rights reserved.
doi:10.1016/j.ijsolstr.2009.09.014

Circular dislocations of general Somigliana type, for which the effective Burgers vector may demonstrate an arbitrary coordinate dependence, were treated by Kolesnikova and Romanov (1986) and Kolesnikova and Romanov (1987), who, in particular, calculated elastic fields of a circular radial disclination loop. For such a loop Burgers vector in radial direction was linearly dependent on the radial coordinate inside the cut path bounded by the defect line, see also (Kolesnikova and Romanov, 2003, 2004). Demir et al. (1992a,b,c, 1993), investigated a Somigliana ring dislocation having prismatic and radial components. In their considerations an effective Burgers vector was defined at the cylindrical cut surface bounded by the circular defect line. Later Korsunsky (1996a), derived the solutions for the elastic fields of Somigliana ring dislocation via Pupkovich-Neuber potential functions. Recently the effect of the position of the cut path on the elastic fields of Somigliana ring dislocation was investigated by Paynter et al. (2007).

Circular loop defects near a free surface, a planar phase boundary or in a plate were studied for a prismatic dislocation loop (Chou, 1963; Baštecká, 1964; Salamon and Dundurs, 1971; Dundurs and Salamon, 1972; Kolesnikova and Romanov, 2004) and a glide dislocation loop (Salamon and Dundurs, 1971; Salamon and Dundurs, 1977), a twist disclination loop (Chou, 1971; Kuo and Mura, 1972b; Kuo et al., 1973; Kolesnikova and Romanov, 2003) and a wedge disclination loop (Kuo and Mura, 1972b), and Somigliana ring dislocation (Korsunsky, 1996b; Paynter and Hills, 2009). Salamon (1981), gave the elastic field for circular a glide dislocation loop laying on the interface of dissimilar materials. In all above works the plane of the loop was assumed to be parallel to free surface or interface. The influence of loop orientation with respect to a free surface or interface was studied for defects with infinitesimally small area. The first solution in integral form was given by Steketee (1958). After that the analytical formulas for elastic fields of infinitesimally small dislocation loops were found by Groves and Bacon (1970) and Bacon and Groves (1970), in case of a semi-infinite elastic media, and by Salamon and Dundurs (1971), in case of two-phase elastic media. Interaction forces of small loops with a free surface were studied by Tikhonov (1967) and Vagera (1970a,b) for the case of an interface. For small twist and wedge disclination loops the asymptotes of elastic fields and interaction forces were provided by Chou and Lu (1972, 1973).

In case of non-planar geometry of involved free surface or interface the list of obtained solutions for elastic fields of circular dislocations and disclinations is much shorter. For a prismatic dislocation loop the stress field and self-energy was found for a coaxial loop in a one-phase cylinder by Ovidko and Sheinerman (2004), and a two-phase cylinder by Aifantis et al. (2007). Recently elastic fields and energy of a prismatic dislocation loop in a cylinder were recalculated by Cai and Weinberger (2009). In case of spherical geometry, a detailed solution for displacement field of a prismatic circular dislocation loop in isotropic elastic sphere was shown by Willis et al. (1983). Later Gryaznov et al. (1991) and Bondarenko and Litoshenko (1997), reported on the results for prismatic loop placed in the media with a spherical phase boundary. For twist disclination loops only one example of solutions for a coaxial cylindrical geometry was published by Kolesnikova and Romanov (2004).

As it was already mentioned, elastic fields of circular dislocation and disclination loops can be used as effective tools in construction of other elasticity solutions for infinite and bounded elastic media. To find solutions of axisymmetric boundary-value problems in an elastic half-space, in a plate of finite thickness, in a general multi-layer planar system, or in a layered cylinder we have proposed virtual circular dislocation–disclination loops technique (Kolesnikova and Romanov, 1986, 2003, 2004). Applying this technique a number of boundary-value elasticity problems for defects have been studied. They include not only the tasks for dislocation and disclination loops but the solutions for screw and edge dislocations and wedge disclinations normal to the surfaces of the plate of finite thickness (Kolesnikova and Romanov, 1986, 1987, 2003), and for a dilatational inclusion in the plate (Kolesnikova and Romanov, 2004). In addition, the virtual defect technique was tested in the solution of contact elasticity problems (Kolesnikova, 2005).

In virtual defect technique the boundary conditions are formulated in terms of unknown distributions of virtual circular dislocation and disclination loops. The obtained integral equations are solved in a standard way by applying integral Hankel-Bessel and Fourier transforms. In such a procedure, equilibrium equations (or Papkovich-Neuber equations) are automatically fulfilled. The helpfulness of the techniques in case of planar and cylindrical interfaces or surfaces is facilitated by a special representation of elastic fields of circular loop defects in terms of Lipschitz-Hankel integrals (LHIs) that include the product of two Bessel functions, an exponential and a power terms as integrands. For the first time the representation of the fields of prismatic dislocation loops via superposition LHIs was shown by Kroupa (1960). Later the displacements, strains and stresses of circular dislocation, disclination and radial Somigliana dislocation loops were presented as superposition of LHIs (e.g. Salamon and Dundurs, 1971; Kolesnikova and Romanov, 1986; Povstenko and Matkovski, 2000).

The next step in the development of virtual dislocation–disclination defects technique is its application to the elasticity problems with spherical symmetry and boundary conditions given on a sphere or a part of a sphere. To approach such problems the method of spherical harmonics is known (Lurie, 1970), in which harmonic functions, and therefore, displacements and stresses are presented in the forms of series with Legendre polynomials with unknown coefficients. Then boundary conditions also need to be written in the form of series with Legendre polynomials but with known coefficients. This procedure allows one to determine the elastic fields. Using such a method the boundary-value problems for screw dislocation and wedge disclination in a spherical particle (Polonsky et al., 1991a,b) have been solved. In the most perfect way this method was demonstrated by Willis et al. (1983), when studying the task on distortions induced by a prismatic dislocation loop in an elastic sphere. In the present work we extend the technique of virtual dislocation–disclination loops to the axial symmetrical elasticity problems with spherically imposed boundary conditions. The first milestone in this direction is the representation of dislocation and disclination loop elastic fields in terms of spherical harmonics. Such representation will be useful in other applications utilizing the properties of circular defects.

The definition of Lipschitz-Hankel integrals (LHIs) is given in Section 2, where it is shown how these special functions appear in elastic fields of circular defect loops. Then representations of the fields of twist disclination loop and prismatic dislocation loop in cylindrical and spherical coordinates are provided. New representations for spherical coordinates are obtained via expansion of LHIs in series with Legendre polynomials. The details and properties of such expansion for LHIs are described in Appendices A and B. Section 3 presents the general scheme of the application of virtual dislocation–disclination loops technique to spherical symmetry. Previously unknown solutions for a twist disclination loop in a spheroid and near a pore are delivered together with alternative solution for a screw dislocation in a spheroid. In Section 4 we demonstrate the possibility of simple calculations of elastic field for a segmented inclusion with uniaxial dilatation. The solution was obtained by exploring the representation of elastic fields of prismatic dislocation loops in terms with Legendre polynomials. Finally in Section 5 we briefly summarize the results.

We believe that ideas and approaches given below can be used in the analysis of a wide spectrum of elasticity problems for the

bodies containing defects and interfaces of a different kind. In particular, the solutions for dislocation loops distributed on spherical surfaces will be important for the analysis of cracks of a complex shape. The solutions of boundary value problems found with the help of virtual dislocation–disclination loops technique can be used as a benchmark for comparison with the results of other numerical methods, e.g. finite element method (FEM). The technique of virtual dislocation–disclination loops can be modified for boundary-value problems of different geometry by using expansions of loop defect elastic fields in various coordinate systems, for example in toroidal coordinates. Finally, the solutions of anisotropic elasticity can be probed with the technique of virtual dislocation–disclination loops.

2. Elastic fields of circular dislocation and disclination loops

In our study of circular defect loops we will analyze twist disclination loops and prismatic dislocation loops. Twist disclination loop is characterized by Frank vector $\boldsymbol{\omega}$ (or vector of rotation), which is an axial vector; it is normal to the loop plane and goes through the center of the circle. Prismatic dislocation loop is characterized by Burgers vector **b** (or vector of translation), which is true vector; it is also normal to the loop plane. Twist disclination loops with opposite direction of Frank vector in structureless continuum are physically undistinguishable, whereas prismatic dislocation loops can be of interstitial or vacancy type depending of mutual orientation of Burgers vector and dislocation line direction.

Three coordinate systems are used: Cartesian (x, y, z), cylindrical (r, φ, z) and spherical (R, θ, φ) shifted with respect to the centre of the defect circle, as shown in Fig. 1. Loop radius is designated as c. The shift z_0 defines the spherical radius $R_0 = \sqrt{c^2 + z_0^2}$, which serves as an important parameter in the given below formulas for elastic fields of circular dislocation and disclination loops.

It is well known that in infinite isotropic elastic media elastic fields of straight linear dislocations and disclinations can be expressed via elementary functions (see, e.g. Hirth and Lothe, 1982; Romanov and Vladimirov, 1992). For circular dislocations and disclinations this is not the case. However the circular geometry and axial symmetry involved dictate that harmonic functions of elasticity problems, total displacements and elastic fields of dislocation and disclination loops can be found in the terms of special functions, i.e. elliptic integrals or Lipschitz-Hankel integrals (LHIs). These representations are appropriate for cylindrical coordinates (see Section 2.1), whereas for spherical coordinates a new representation is needed, as will be given in Section 2.2.

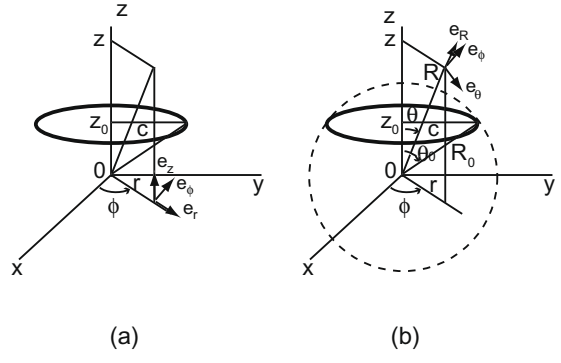

Fig. 1. Schematics of circular defect of radius c in infinite elastic media. (a) Circular loop contour shifted by z_0 with respect to the origin of cylindrical coordinate system (r, φ, z); unit basis vectors $\mathbf{e}_r, \mathbf{e}_\varphi, \mathbf{e}_z$ are shown. (b) Circular loop contour shifted with respect to origin of spherical coordinate system(R, θ, φ); unit basis vectors $\mathbf{e}_R, \mathbf{e}_\theta, \mathbf{e}_\varphi$ are shown. Dashed circle defines a sphere of radius R_0 used in expansion of Lipschitz-Hankel integrals in series with Legendre polynomials (see below).

2.1. Representation via cylindrical functions

2.1.1. Lipschitz-Hankel integrals (LHIs)

Lipschitz-Hankel integrals are defined as improper integrals from zero to infinity with integrands consisting of the product of one or several Bessel functions, exponential function and power function (see, for example, Watson, 1944). In case of two Bessel functions with indexes μ and ν and power function with the exponent λ the following notation (Eason et al., 1955) for LHIs is used:

$$J(\mu, \nu; \lambda) = \int_0^\infty J_\mu(\kappa) J_\nu(\rho\kappa) e^{-\zeta\kappa} \kappa^\lambda d\kappa. \tag{1}$$

These integrals depend on two parameters ζ and ρ. In the simplest case the indexes μ, ν, and λ in LHIs are real numbers. Lipschitz-Hankel integrals converge for $\zeta > 0$ and$\mu + \nu + \lambda > -1$. If $\zeta = 0$ the convergence condition for indexes becomes: (i) $\mu + \nu + 1 > -\lambda > -1$ at $\rho \neq 1$, (ii) $\mu + \nu + 1 > -\lambda > 0$ at $\rho = 1$. Lipschitz-Hankel integrals of type given by Eq. (1) have been investigated in details by Eason et al. (1955), where representations of LHIs via complete elliptic integral functions were shown, some approximate formulas for LHIs for small ρ or $\rho \cong 1$ and small ζ were given, and recurrence relations among LHIs having close indexes μ, ν and λ were presented. Later the limits of LHIs with integer indexes $J(m, n; p)$ at $\zeta - > 0$ were analyzed in full details (Salamon and Walter, 1979). Such features, as the Heaviside step function like behavior for some LHIs at $\zeta = 0$ and their δ-function like character at $\zeta = 0$, $\rho = 1$ were revealed and proved.

Integrals $J(m, n; p)$ with integer indexes are involved in the expressions for the coordinate dependences of the fields of circular dislocation and disclination loops with the following parameters: $\rho = \frac{r}{c}$; $\zeta = \frac{|z - z_0|}{c}$, where c is a radius of loop, z_0 is coordinate of the loop in a cylindrical coordinate system (r, φ, z) (Fig. 1a).

2.1.2. Twist disclination loop

For the first time the elastic fields of a twist disclination loop (TL) were derived by Owen and Mura (1967), where the non-zero stress tensor components in cylindrical coordinate were written in terms of complete elliptic integrals. Later the fields of TL were presented by Kuo and Mura (1972b) in terms of LHIs. Here we follow the results given by Kolesnikova and Romanov (2004).

To obey the sign convention for disclination Frank vector one has to choose first the direction of the disclination line, for example as $\mathbf{l} = \mathbf{e}_\varphi$, where $\mathbf{e}_\varphi$ is unit vector related to coordinate φ. Then for the TL with Frank vector $\boldsymbol{\omega} = -\omega\mathbf{e}_z$, where ω is a disclination strength and $\mathbf{e}_z$ is another unit vector, the fields of displacements u_j and stresses σ_{ij} can be written as:

$$u_r^{TL} = u_z^{TL} = 0, \tag{2a, b}$$

$$u_\varphi^{TL} = \frac{\omega c \,\mathrm{sgn}(z - z_0)}{2} J(2, 1; 0), \tag{2c}$$

$$\sigma_{r\varphi}^{TL} = -\frac{G\omega \,\mathrm{sgn}(z - z_0)}{2} J(2, 2; 1), \tag{3a}$$

$$\sigma_{z\varphi}^{TL} = -\frac{G\omega}{2} J(2, 1; 1), \tag{3b}$$

$$\sigma_{rr}^{TL} = \sigma_{\varphi\varphi}^{TL} = \sigma_{zz}^{TL} = \sigma_{rz}^{TL} = 0, \tag{3e, f}$$

where G is shear modulus; ν is Poisson ratio, and $\mathrm{sgn}(z - z_0) = \begin{cases} 1, & z > z_0 \\ -1, & z < z_0 \end{cases}$.

2.1.3. Prismatic dislocation loop

Already in the first publication devoted to the calculation of elastic fields of a prismatic dislocation loop (PL) Kroupa used the

forms with LHIs (but in slightly different notation, see Kroupa, 1960), which were expressed via elliptic integrals for the sake of numerical calculations. Later the notation with LHIs for elastic fields of PLs became widely accepted (e.g. Dundurs and Salamon, 1972; Kolesnikova and Romanov, 1986; Povstenko, 1995).

Prismatic loop with line direction $\mathbf{l} = \mathbf{e}_\varphi$ and Burgers vector $\mathbf{b} = -b\mathbf{e}_\mathbf{z}$, where b is the magnitude of Burgers vector, is of interstitial type. For such PL in the geometry shown in Fig. 1a displacements u_j and stressesσ_{ij} are:

$$u_r^{PL} = \frac{b}{4(1-\nu)}\left[(2\nu-1)J(1,1;0) + \frac{|z-z_0|}{c}J(1,1;1)\right], \tag{4a}$$

$$u_\varphi^{PL} = 0, \tag{4b}$$

$$u_z^{PL} = \frac{b\,\mathrm{sgn}(z-z_0)}{4(1-\nu)}\left[2(1-\nu)J(1,0;0) + \frac{|z-z_0|}{c}J(1,0;1)\right], \tag{4c}$$

$$\sigma_{rr}^{PL} = \frac{Gb}{2(1-\nu)}\left[\frac{1-2\nu}{r}J(1,1;0) + \frac{|z-z_0|}{c^2}J(1,0;2) - \frac{1}{c}J(1,0;1) - \frac{|z-z_0|}{cr}J(1,1;1)\right], \tag{5a}$$

$$\sigma_{\varphi\varphi}^{PL} = \frac{Gb}{2(1-\nu)}\left[\frac{2\nu-1}{r}J(1,1;0) - \frac{2\nu}{c}J(1,0;1) + \frac{|z-z_0|}{cr}J(1,1;1)\right], \tag{5b}$$

$$\sigma_{zz}^{PL} = \frac{-Gb}{2(1-\nu)}\left[\frac{1}{c}J(1,0;1) + \frac{|z-z_0|}{c^2}J(1,0;2)\right], \tag{5c}$$

$$\sigma_{rz}^{PL} = \frac{-Gb}{2(1-\nu)}\cdot\frac{(z-z_0)}{c^2}J(1,1;2), \tag{5d}$$

$$\sigma_{r\varphi}^{PL} = \sigma_{z\varphi}^{PL} = 0, \tag{5e,f}$$

Here the designations are similar to those used in Eqs. (2) and (3).

2.2. Representation via spherical functions

It is well-known that solutions of elasticity problems in spherical coordinates are simplified by using representations with spherical harmonics, i.e. expansions with Legendre polynomials (Lurie, 1970; Love, 2003), in which variables R, θ, φ are separated. One way to find the elastic fields and dislocation and disclination loops in terms of spherical functions is the direct solution of elasticity problem using general elasticity approaches with the boundary conditions given on a spherical surface. Such techniques were applied by Willis et al. (1983) and Bondarenko and Litoshenko (1997). The other way is to use known expressions for loop elastic fields, e.g. given by Eqs. (2)–(5) with corresponding representation of LHIs via spherical functions. To achieve this, a mathematical problem of the expansion of LHIs into the series with Legendre polynomials has to be solved. Appendices A and B present such solutions for LHIs $J(m, n; p)$ with integer indexes m, n, and p. When LHI expansions are known dislocation and disclination loop elastic fields can be written in terms of Legendre polynomials.

In addition, components of displacements and stresses must be transformed from cylindrical (r, φ, z) to spherical (R, θ, φ) coordinates in an obvious manner:

$$u_R = u_r\sin\theta + u_z\cos\theta, \tag{6a}$$

$$u_\theta = u_r\cos\theta - u_z\sin\theta, \tag{6b}$$

$$u_\varphi = u_\varphi, \tag{6c}$$

$$\sigma_{RR} = \sigma_{rr}\sin^2\theta + \sigma_{zz}\cos^2\theta + 2\sigma_{rz}\sin\theta\cos\theta, \tag{7a}$$

$$\sigma_{\theta\theta} = \sigma_{rr}\cos^2\theta + \sigma_{zz}\sin^2\theta - 2\sigma_{rz}\sin\theta\cos\theta, \tag{7b}$$

$$\sigma_{\varphi\varphi} = \sigma_{\varphi\varphi}, \tag{7c}$$

$$\sigma_{R\theta} = (\sigma_{rr} - \sigma_{zz})\sin\theta\cos\theta + \sigma_{rz}(\cos^2\theta - \sin^2\theta), \tag{7d}$$

$$\sigma_{R\varphi} = \sigma_{r\varphi}\sin\theta + \sigma_{z\varphi}\cos\theta. \tag{7e}$$

$$\sigma_{\theta\varphi} = \sigma_{r\varphi}\cos\theta - \sigma_{z\varphi}\sin\theta, \tag{7f}$$

In the following Legendre expansions for LHIs involved into fields of TL and PL are presented for two regions $R > R_0$ and at $R < R_0$, where R_0 is a radius of expansion shown in Fig. 1b.

2.2.1. Twist disclination loop

From Eqs. (2), (3), (6), and (7) and with the help of expansions for LHIs given by Eqs. (A10h,i,k) the displacements and stresses of a TL are found as:

$$u_R^{TL} = u_\theta^{TL} = 0 \tag{8a,b}$$

$$u_\varphi^{TL} = \frac{\omega R_0}{2}\begin{cases} (-1)\sum_{k=2}^{\infty}\frac{1}{k(k+1)(k+2)}\left(\frac{R_0}{R}\right)^{k+1}P_k^2(\cos\theta_0)\sin^2\theta_0 P_k^1(\cos\theta), & R_0 < R \\ \left(\frac{\mathrm{sgn}(z-z_0)R\sin\theta}{R_0} + \frac{R}{R_0}\left(\cos\theta_0 + \frac{1}{4}\sin 2\theta_0\sin\theta_0\right)\sin\theta\right. & \\ \left. +\sum_{k=2}^{\infty}\frac{1}{(k-1)k(k+1)}\left(\frac{R}{R_0}\right)^{k}P_k^2(\cos\theta_0)\sin^2\theta_0 P_k^1(\cos\theta)\right), & R < R_0 \end{cases} \tag{8c}$$

$$\sigma_{R\varphi}^{TL} = \frac{-G\omega}{2}\begin{cases} \sum_{k=2}^{\infty}\frac{1}{(k+1)(k+2)}\left(\frac{R_0}{R}\right)^{k+2}P_k^2(\cos\theta_0)\sin^2\theta_0\left[\frac{1}{k}P_{k+1}^2(\cos\theta)\sin\theta - P_{k+1}^1(\cos\theta)\cos\theta\right], & R_0 < R \\ (-1)\sum_{k=1}^{\infty}\frac{1}{k(k+1)}\left(\frac{R}{R_0}\right)^{k}P_{k+1}^2(\cos\theta_0)\sin^2\theta_0\left[\frac{1}{k+2}P_k^2(\cos\theta)\sin\theta + P_k^1(\cos\theta)\cos\theta\right], & R < R_0 \end{cases} \tag{9a}$$

$$\sigma_{\theta\varphi}^{TL} = \frac{-G\omega}{2}\begin{cases} \sum_{k=2}^{\infty}\frac{1}{(k+1)(k+2)}\left(\frac{R_0}{R}\right)^{k+2}P_k^2(\cos\theta_0)\sin^2\theta_0\left[\frac{1}{k}P_{k+1}^2(\cos\theta)\cos\theta + P_{k+1}^1(\cos\theta)\sin\theta\right], & R_0 < R \\ (-1)\sum_{k=1}^{\infty}\frac{1}{k(k+1)}\left(\frac{R}{R_0}\right)^{k}P_{k+1}^2(\cos\theta_0)\sin^2\theta_0\left[\frac{1}{k+2}P_k^2(\cos\theta)\cos\theta - P_k^1(\cos\theta)\sin\theta\right], & R < R_0 \end{cases} \tag{9b}$$

$$\sigma_{RR}^{TL} = \sigma_{\theta\theta}^{TL} = \sigma_{\varphi\varphi}^{TL} = \sigma_{R\theta}^{TL} = 0, \tag{9c–f}$$

where $P_n^1(t)$ and $P_n^2(t)$ are associated Legendre polynomials, which are defined with the help of Legendre polynomials $P_n(t)$ via $P_n^m(t) = (-1)^m(1-t^2)^{\frac{m}{2}}\frac{d^m}{dt^m}P_n(t), m = 1, 2, 3\ldots$ (see, e.g. Bateman and Erdélyi, 1953).

Representation of TL displacements in terms of Legendre polynomials Eq. (8c) permits us to extract the displacement jump in the plane of the loop:

$$\left[u_\varphi^{TL}\right]\Big|_{z=z_0} = u_\varphi^{TL}\Big|_{\substack{R<R_0,\\ z=z_0+\delta}} - u_\varphi^{TL}\Big|_{\substack{R<R_0,\\ z=z_0-\delta}} = \omega r H\Big(1-\frac{r}{c}\Big), \tag{10}$$

where $H(1-\frac{r}{c})$ is the Heaviside step function. Analysis shows that the first term in the expansion Eq. (8c) at $R < R_0$ is responsible for the jump. This gives the possibility to subdivide total displacements into elastic and plastic parts explicitly.

$$\frac{1}{k}P_{k+1}^2(\cos\theta)\cos\theta + P_{k+1}^1(\cos\theta)\sin\theta = \frac{1}{k}P_k^2(\cos\theta), \tag{11c}$$

$$\frac{1}{k+2}P_k^2(\cos\theta)\cos\theta - P_k^1(\cos\theta)\sin\theta = \frac{1}{k+2}P_{k+1}^2(\cos\theta), \tag{11d}$$

As a result non-vanished stress components of a TL expressed in terms of spherical harmonics can be written in a compact form:

$$\sigma_{R\varphi}^{TL} = \frac{-G\omega}{2}\begin{cases} (-1)\sum_{k=2}^{\infty}\frac{1}{k(k+1)}\left(\frac{R_0}{R}\right)^{k+2}P_k^2(\cos\theta_0)\sin^2\theta_0 P_k^1(\cos\theta), & R_0 < R \\ (-1)\sum_{k=1}^{\infty}\frac{1}{(k+1)(k+2)}\left(\frac{R}{R_0}\right)^{k}P_{k+1}^2(\cos\theta_0)\sin^2\theta_0 P_{k+1}^1(\cos\theta), & R < R_0 \end{cases}, \tag{12a}$$

$$\sigma_{\theta\varphi}^{TL} = \frac{-G\omega}{2}\begin{cases} \sum_{k=2}^{\infty}\frac{1}{k(k+1)(k+2)}\left(\frac{R_0}{R}\right)^{k+2}P_k^2(\cos\theta_0)\sin^2\theta_0 P_k^2(\cos\theta), & R_0 < R \\ (-1)\sum_{k=1}^{\infty}\frac{1}{k(k+1)(k+2)}\left(\frac{R}{R_0}\right)^{k}P_{k+1}^2(\cos\theta_0)\sin^2\theta_0 P_{k+1}^2(\cos\theta), & R < R_0 \end{cases}. \tag{12b}$$

It is useful to note that the formulas of Eq. (9) can be written in series with Legendre polynomials $P_k^1(\cos\theta)$ only and without additional multipliers $\cos\theta$ and $\sin\theta$, see expressions in square brackets. Using the recurrence relations $\sqrt{1-t^2}P_n^2(t) = \frac{1}{2n+1}\left[(n-1)nP_{n+1}^1(t) - (n+1)(n+2)P_{n-1}^1(t)\right]$, $tP_n^1(t) = \frac{1}{2n+1}\left[nP_{n+1}^1(t) + (n+1)P_{n-1}^1(t)\right]$, $\sqrt{1-t^2}P_n^1(t) = \frac{1}{2n+1}\left[P_{n-1}^2(t) - P_{n+1}^2(t)\right]$, $tP_n^2(t) = \frac{1}{2n+1}\left[(n-1)P_{n+1}^2(t) + (n+2)P_{n-1}^2(t)\right]$ (Bateman and Erdélyi, 1953), one finds:

$$\frac{1}{k}P_{k+1}^2(\cos\theta)\sin\theta - P_{k+1}^1(\cos\theta)\cos\theta = -\frac{(k+2)}{k}P_k^1(\cos\theta), \tag{11a}$$

$$\frac{1}{k+2}P_k^2(\cos\theta)\sin\theta + P_k^1(\cos\theta)\cos\theta = \frac{k}{k+2}P_{k+1}^1(\cos\theta), \tag{11b}$$

2.2.2. Prismatic dislocation loop

Elastic fields of a PL can be also found in the form of the components in spherical coordinates. However these components are rather cumbersome and for the aim of the present study such a representation is not necessary. In the following (see Section 4) we demonstrate how the solutions for PLs can be used for the construction of the elastic fields of segmented spherical inclusion with uniaxial eigenstrain. To achieve this aim the components of PL fields can be given in any coordinate system but they should be expressed via spherical coordinate variables under the condition of variable separation, i.e. in terms of Legendre polynomials.

The components of PL displacement field in cylindrical coordinates are found from Eq. (4) and expansions (A10a,b,d,e):

$$u_r^{PL} = \frac{b}{4(1-\nu)}\begin{cases} \Big((2\nu-1)\sin\theta_0\sum_{k=1}^{\infty}\frac{1}{k(k+1)}\left(\frac{R_0}{R}\right)^{k+1}P_k^1(\cos\theta_0)P_k^1(\cos\theta) \\ +\frac{(R\cos\theta - R_0\cos\theta_0)}{R_0}\sin\theta_0\sum_{k=1}^{\infty}\frac{1}{(k+1)}\left(\frac{R_0}{R}\right)^{k+2}P_k^1(\cos\theta_0)P_{k+1}^1(\cos\theta)\Big), & R_0 < R \\ \Big((2\nu-1)\sin\theta_0\sum_{k=1}^{\infty}\frac{1}{k(k+1)}\left(\frac{R}{R_0}\right)^{k}P_k^1(\cos\theta_0)P_k^1(\cos\theta) \\ -\frac{(R\cos\theta - R_0\cos\theta_0)}{R_0}\sin\theta_0\sum_{k=1}^{\infty}\frac{1}{(k+1)}\left(\frac{R}{R_0}\right)^{k}P_{k+1}^1(\cos\theta_0)P_k^1(\cos\theta)\Big), & R < R_0 \end{cases} \tag{13a}$$

$$u_\varphi^{PL} = 0, \tag{13b}$$

$$u_z^{PL} = \frac{b}{4(1-\nu)}\begin{cases} \Big(-2(1-\nu)\sin\theta_0\sum_{k=1}^{\infty}\frac{1}{(k+1)}\left(\frac{R_0}{R}\right)^{k+1}P_k^1(\cos\theta_0)P_k(\cos\theta) - \\ -\frac{(R\cos\theta - R_0\cos\theta_0)}{R_0}\sin\theta_0\sum_{k=1}^{\infty}\left(\frac{R_0}{R}\right)^{k+2}P_k^1(\cos\theta_0)P_{k+1}(\cos\theta)\Big), & R_0 < R \\ \Big(2(1-\nu)\mathrm{sgn}(z-z_0) + (1-\nu)\cos\theta_0 + (1-\nu)\sin\theta_0\sum_{k=1}^{\infty}\frac{1}{k}\left(\frac{R}{R_0}\right)^{k}P_k^1(\cos\theta_0)P_k(\cos\theta) - \\ -\frac{(R\cos\theta - R_0\cos\theta_0)}{R_0}\sin\theta_0\sum_{k=0}^{\infty}\left(\frac{R}{R_0}\right)^{k}P_{k+1}^1(\cos\theta_0)P_k(\cos\theta)\Big), & R < R_0 \end{cases} \tag{13c}$$

Similarly to the case of a TL, the first term in Eq. (13c) at $R < R_0$ is responsible for the displacement jump:

$$\left[u_z^{PL}\right]\big|_{z=z_0} = u_z^{PL}\big|_{\substack{R<R_0,\\ z=z_0+\delta}} - u_z^{PL}\big|_{\substack{R<R_0,\\ z=z_0-\delta}} = bH\left(1-\frac{r}{c}\right) \tag{14}$$

The procedure of the LHI expansion in the series with Legendre polynomials can be performed in the expressions for cylindrical components of PL stress tensor, i.e. in Eq. (5). Here as an example we give only two components, which are relatively simple and concise in notation:

$$\sigma_{zz}^{PL} = \frac{-Gb}{2(1-\nu)R_0}\begin{cases} \Big(-\sin\theta_0\sum_{k=1}^{\infty}\left(\frac{R_0}{R}\right)^{k+2}P_k^1(\cos\theta_0)P_{k+1}^1(\cos\theta) \\ -\frac{(R\cos\theta-R_0\cos\theta_0)}{R_0}\sin\theta_0\sum_{k=1}^{\infty}(k+2)\left(\frac{R_0}{R}\right)^{k+3}P_k^1(\cos\theta_0)P_{k+2}(\cos\theta)\Big), & R_0 < R \\ \Big(-\sin\theta_0\sum_{k=0}^{\infty}\left(\frac{R}{R_0}\right)^{k}P_{k+1}^1(\cos\theta_0)P_k(\cos\theta) \\ +\frac{(R\cos\theta-R_0\cos\theta_0)}{R_0}\sin\theta_0\sum_{k=0}^{\infty}(k+1)\left(\frac{R}{R_0}\right)^{k}P_{k+2}^1(\cos\theta_0)P_k(\cos\theta)\Big), & R < R_0 \end{cases} \tag{15a}$$

$$\sigma_{rz}^{PL} = \frac{-Gb}{2(1-\nu)R_0}\begin{cases} \frac{(R\cos\theta-R_0\cos\theta_0)}{R_0}\sin\theta_0\sum_{k=1}^{\infty}\left(\frac{R_0}{R}\right)^{k+3}P_k^1(\cos\theta_0)P_{k+2}^1(\cos\theta), & R_0 < R \\ \frac{(R\cos\theta-R_0\cos\theta_0)}{R_0}\sin\theta_0\sum_{k=1}^{\infty}\left(\frac{R}{R_0}\right)^{k}P_{k+2}^1(\cos\theta_0)P_k^1(\cos\theta), & R < R_0 \end{cases} \tag{15b}$$

In the derivation of these formulas, Eqs. 5c and 5d and Eqs. (A10b,c,f) were exploited.

3. Boundary-value problems for defects in elastic media with spherical boundaries

3.1. Method of virtual dislocation–disclination loops

Elastic fields of disclination and dislocation loops written in terms of Legendre polynomials provide a unique possibility for solution of axisymmetric elasticity boundary-value problems for defects in presence of spherical free surfaces and interfaces.

Two classes of boundary-value problems can be considered:

(i) spheroid or spherical void with traction-free spherical surface with conditions for stress tensor components:

$$\sigma_{Rj}\big|_{R=a} = 0, \quad (j = R, \theta, \varphi) \tag{16}$$

where a is a spheroid or pore radius.

(ii) spherical boundary between elastically dissimilar phases I (inclusion) and II (matrix) with continuity conditions for displacements and stresses:

$$u_j^I\Big|_{R=a} = u_j^{II}\Big|_{R=a}, \tag{17a}$$

$$\sigma_{Rj}^I\Big|_{R=a} = \sigma_{Rj}^{II}\Big|_{R=a}, \quad (j = R, \theta, \varphi) \tag{17b}$$

The elastic field of a defect placed in the vicinity of one of the above spherical surfaces, is constructed as a sum of the defect elastic field in an infinite medium and an addition field due to distributions of the virtual dislocation–disclination loops. In the most general case the boundary conditions Eq. (16) will constitute the system of six equations. Therefore six independent distributions of virtual dislocation–disclination loops should be involved. Three of these distributions are placed in matrix II with their elastic fields acting in the phase I (spheroid) interior. Three remaining distributions are placed inside spheroid I with their fields acting in phase II (matrix). For free surface boundary conditions of Eq. (16) only three virtual dislocation–disclination distributions are necessary. Actual choice of the type of defects for virtual distributions depends on the properties of symmetry for elastic fields of the original defect. Important is the condition that virtual defect distributions are placed outside the region in which their elastic fields act.

Boundary conditions of Eq. (16) or Eq. (17) written in terms of virtual dislocations and disclinations become the integral equations for unknown functions of loop distributions. In case of planar and cylindrical surfaces and interfaces the integral equations can be transformed to algebraic equations with respect to transformers of functions of distributions. Previously we have solved a set of axisymmetric elasticity problems for defects in plates with planar surfaces (Kolesnikova and Romanov, 1986, 1987, 2003, 2004); to get these solutions Hankel-Bessel integral transformation was used. The other solved axisymmetric problems operate with cylindrical system, where the Fourier transformation was utilized (for details see Kolesnikova and Romanov, 2004; Aifantis et al., 2007). In the following the axisymmetric boundary conditions for defects in spheroid and at a spherical pore are investigated.

3.2. Twist loop in a spheroid and near a spherical pore

Let us consider axisymmetric elasticity boundary-value problems for a TL with Frank vector $\boldsymbol{\omega} = -\omega\mathbf{e}_z$ and direction of the disclination line $\mathbf{e}_\varphi$, in a spherical particle (Fig. 2a) and near a spherical pore (Fig. 2b). Following general scheme the field of the TL in a particle or near pore is given by the sum of its field in an infinite medium and an image field. The image field is generated by distributions of virtual TLs that are shown schematically by dashed circles in Fig. 2a and b. Note that choice of the radius of sphere $\tilde{R}_0$, at which virtual defects are placed, is arbitrary. As it will be illustrated below this radius does not enter into the final solution of the boundary-value problem.

Applying such a procedure the stresses of a TL in a spheroid ${}^s\sigma_{ij}^{TL}$ or near pore ${}^p\sigma_{ij}^{TL}$ can be written in the following form:

$${}^{s,p}\sigma_{ij}^{TL} = \sigma_{ij}^{TL} + \int_0^{\pi} f(\tilde{\theta}_0)\sigma_{ij}^{TL_v}\tilde{R}_0\sin\tilde{\theta}_0 d\tilde{\theta}_0, \tag{18}$$

where σ_{ij}^{TL} are stresses of real TL in infinite medium (see Eq. (3) or (12)), $\sigma_{ij}^{TL_v}$ are stresses of a probe virtual TL also taken for an infinite medium, $f(\tilde{\theta}_0)$ is the function of virtual TL distribution and $\tilde{R}_0, \tilde{\theta}_0$ are coordinates of a probe TL, see Fig. 2a and b. The stresses given by Eq.

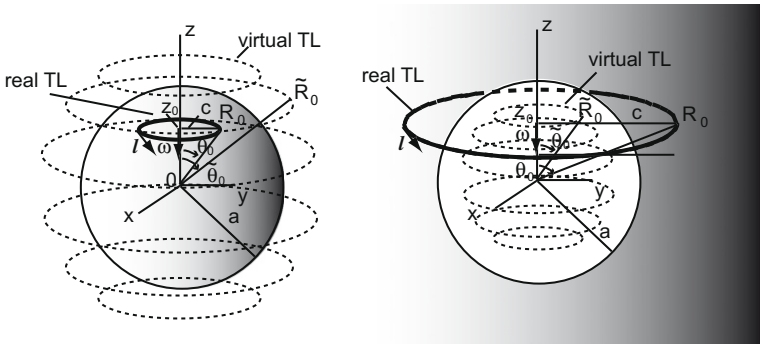

Fig. 2. Twist disclination loop (real TL) in a spherical particle (a) and near a pore (b). Frank vector ω and line direction $\mathbf{l}$ of real TL are shown; R_0, θ_0 are coordinates of real TL. Dashed lines designate virtual twist disclination loops (virtual TLs). $\tilde{R}_0, \tilde{\theta}_0$ are coordinates of a probe virtual TL in the distribution.

(18) at the spheroid (pore) surface must satisfy the boundary conditions of Eq. (16):

$$ {}^{s,p}\sigma^{TL}_{R\varphi}|_{R=a} + \int_0^{\pi} f(\tilde{\theta}_0)\sigma^{TLv}_{R\varphi}|_{R=a}\tilde{R}_0 \sin\tilde{\theta}_0 d\tilde{\theta}_0 = 0. \tag{19}$$

Using the representation of TL stresses in terms of Legendre polynomials (see Eq. (12a)) and assuming the magnitudes of Frank's vector of the real TL and virtual TLs being the same we can rewrite the boundary condition Eq. (19) for TL in spheroid as:

$$\frac{G\omega}{2}\sum_{k=2}^{\infty}\frac{1}{k(k+1)}\left(\frac{R_0}{a}\right)^{k+2}P^2_k(\cos\theta_0)\sin^2\theta_0 P^1_k(\cos\theta) + \frac{G\omega}{2}\sum_{k=1}^{\infty}\frac{1}{(k+1)(k+2)}\left(\frac{a}{\tilde{R}_0}\right)^{k}A_{k+1}P^1_{k+1}(\cos\theta) = 0, \tag{20}$$

where the designation for transform coefficients $A_{k+1} = \int_0^{\pi} f(\tilde{\theta}_0)\tilde{R}_0 \sin^3\tilde{\theta}_0 P^2_{k+1}(\cos\tilde{\theta}_0)d\tilde{\theta}_0$ is introduced. The property of orthogonality for Legendre polynomials straightforward leads to the following results for the coefficients:

$$A_n = -\left(\frac{\tilde{R}_0}{a}\right)^{n-1}\left(\frac{R_0}{a}\right)^{n+2}P^2_n(\cos\theta_0)\sin^2\theta_0, \quad n = 2,3,4,\ldots \tag{21}$$

Finally, Eqs. (12), (18), and (21) give the solution for stresses of a twist disclination loop in an elastic spheroid:

$$ {}^{s}\sigma^{TL}_{R\varphi} = -\frac{G\omega}{2}[\mathrm{sgn}(z-z_0)J(2,2;1)\sin\theta + J(2,1;1)\cos\theta] - \frac{G\omega\sin^2\theta_0}{2}\sum_{k=1}^{\infty}\frac{1}{(k+1)(k+2)}\left(\frac{R_0}{a}\right)^{k+3}\times\left(\frac{R}{a}\right)^{k}P^2_{k+1}(\cos\theta_0)P^1_{k+1}(\cos\theta), \tag{22a}$$

$$ {}^{s}\sigma^{TL}_{\theta\varphi} = -\frac{G\omega}{2}[\mathrm{sgn}(z-z_0)J(2,2;1)\cos\theta - J(2,1;1)\sin\theta] - \frac{G\omega\sin^2\theta_0}{2}\sum_{k=1}^{\infty}\frac{1}{k(k+1)(k+2)}\left(\frac{R_0}{a}\right)^{k+3}\times\left(\frac{R}{a}\right)^{k}P^2_{k+1}(\cos\theta_0)P^2_{k+1}(\cos\theta). \tag{22b}$$

The field ${}^{s}\sigma^{TL}_{ij}$ satisfies (i) boundary conditions (16) and (ii) equations of mechanical equilibrium. In case of the axisymmetric problem for stress tensor with only two components, i.e. $\sigma_{R\varphi}, \sigma_{\theta\varphi}$, there remains a single equilibrium equation $\frac{\partial\sigma_{R\varphi}}{\partial R} + \frac{\partial\sigma_{\theta\varphi}}{R\partial\theta} + \frac{3\sigma_{R\varphi}+2\sigma_{\theta\varphi}\cot\theta}{R} = 0$. The radius of sphere $\tilde{R}_0$, at which virtual defects are placed, does not enter into the solution given Eq. (22).

By analogy to the solution for a TL in a spheroid one can get the solution of elasticity boundary-value problem for a TL near a pore in the geometry shown in Fig. 2b. Accounting for Eq. (12a) boundary condition Eq. (16) can be written as:

$$\frac{G\omega}{2}\sum_{k=1}^{\infty}\frac{1}{(k+1)(k+2)}\left(\frac{a}{R_0}\right)^{k}P^2_{k+1}(\cos\theta_0)\sin^2\theta_0 P^1_{k+1}(\cos\theta) + \frac{G\omega}{2}\sum_{k=2}^{\infty}\frac{1}{k(k+1)}\left(\frac{\tilde{R}_0}{a}\right)^{k+2}A'_k P^1_k(\cos\theta) = 0, \tag{23}$$

from which the coefficients $A'_k = \int_0^{\pi} f(\tilde{\theta}_0)\tilde{R}_0 \sin^3\tilde{\theta}_0 P^2_k(\cos\tilde{\theta}_0)d\tilde{\theta}_0$ can be found:

$$A'_n = -\left(\frac{a}{\tilde{R}_0}\right)^{n+2}\left(\frac{a}{R_0}\right)^{n-1}P^2_n(\cos\theta_0)\sin^2\theta_0, \quad n = 2,3,4,\ldots \tag{24}$$

This result together with Eqs. (12) and (18) allow us to write the stress tensor components of a TL coaxial to a spherical pore:

$$ {}^{p}\sigma^{TL}_{R\varphi} = -\frac{G\omega}{2}[\mathrm{sgn}(z-z_0)J(2,2;1)\sin\theta + J(2,1;1)\cos\theta] - \frac{G\omega\sin^2\theta_0}{2}\sum_{k=2}^{\infty}\frac{1}{k(k+1)}\left(\frac{a}{R}\right)^{k+2}\left(\frac{a}{R_0}\right)^{k-1}\times P^2_k(\cos\theta_0)P^1_k(\cos\theta), \tag{25a}$$

$$ {}^{p}\sigma^{TL}_{\theta\varphi} = -\frac{G\omega}{2}[\mathrm{sgn}(z-z_0)J(2,2;1)\cos\theta - J(2,1;1)\sin\theta] + \frac{G\omega\sin^2\theta_0}{2}\sum_{k=2}^{\infty}\frac{1}{k(k+1)(k+2)}\left(\frac{a}{R}\right)^{k+2}\times\left(\frac{a}{R_0}\right)^{k-1}P^2_k(\cos\theta_0)P^2_k(\cos\theta). \tag{25b}$$

The field ${}^{p}\sigma^{TL}_{ij}$ satisfies boundary conditions and equations of equilibrium.

We have to note that in the case of the derivation of the displacement field of a real defect in an elastic body with boundaries (e.g. twist disclination loop in a spheroid or near a pore) the method of virtual loops can also be successfully applied. However in the displacement solution, the discontinuous terms in the displacement fields of virtual defects, i.e. first term in Eqs. (8c) or (13c), must be omitted. This means that only the displacement contribution of virtual loops, which is responsible for elastic strains, should be taken into account. The other possibility to use the displacement filed of virtual dislocation–disclination loops in the solution of boundary-value problem could be the proper choice of the cut path in the procedure of the creation of virtual loop defects. For

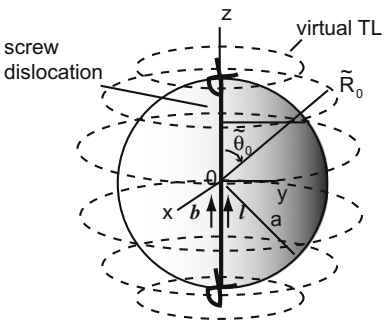

Fig. 3. Screw dislocation in elastic spheroid. Burgers vector **b** and line direction ***l*** of dislocation are shown. Dashed lines designate the virtual twist disclination loops (virtual TLs). $\tilde{R}_0, \tilde{\theta}_0$ are coordinates of a probe virtual TL in the distribution.

example, in the solution for a TL near a pore the virtual loops having the cut path in the internal areas of the loop contours and distributed inside the pore will produce no additional discontinuities outside the pore. In the same manner, for finding the displacement field of a defect inside a spheroid, virtual loops can be placed outside the spheroid with their cut paths being in the external areas of the loop contours.

3.3. Screw dislocation in a spheroid

The elasticity boundary-value problem for a screw dislocation laying along the diameter of a spherical particle as it is shown in Fig. 3 was solved by Polonsky et al. (1991a). Here we apply the method of virtual disclination loops to get this known solution.

The field of the dislocation in spheroid is represented as the sum of the elastic field σ^0_{ij} of dislocation in infinite medium and an image field σ^i_{ij}. The field σ^i_{ij} is the superposition of the elastic fields caused by the distribution of virtual TLs (Fig. 3):

$$\sigma^i_{R\varphi} = \int_0^\pi \psi(\tilde{\theta}_0)\sigma^{TL_V}_{R\varphi}\tilde{R}_0 \sin\tilde{\theta}_0 d\tilde{\theta}_0, \tag{26}$$

where $\psi(\tilde{\theta}_0)$ is the function of loop distribution, $\tilde{R}_0, \tilde{\theta}_0$ are the coordinates of a probe virtual TL in the distribution (Fig. 3).

Non-zero stress components for a screw dislocation with Burgers vector $\mathbf{b} = b\mathbf{e_z}$ in infinite medium in spherical coordinate system can be easily obtained from well-known expressions for stresses in cylindrical coordinates (e.g. Hirth and Lothe, 1982):

$$\sigma^0_{R\varphi} = \frac{Gb}{2\pi R}\cot\theta, \tag{27a}$$

$$\sigma^0_{\theta\varphi} = -\frac{Gb}{2\pi R}. \tag{27b}$$

With the help of image stresses from virtual TL distribution the boundary conditions Eq. (16) become:

$$\sigma^0_{R\varphi}|_{R=a} + \int_0^\pi \psi(\tilde{\theta}_0)\sigma^{TL}_{R\varphi}|_{R=a}\tilde{R}_0 \sin\tilde{\theta}_0 d\tilde{\theta}_0 = 0. \tag{28}$$

Taking into account Eq. (12a) and the expansion of $\cot\theta$ in Legendre series we can rewrite Eq. (28) in the form containing Legendre polynomials:

$$-\frac{Gb}{2\pi a}\sum_{m=1}^{\infty}\frac{(4m+1)}{2m(2m+1)}P^1_{2m}(\cos\theta) + \frac{G\omega}{2}\sum_{k=1}^{\infty}\frac{1}{(k+1)(k+2)}\left(\frac{a}{\tilde{R}_0}\right)^k B_{k+1}P^1_{k+1}(\cos\theta) = 0, \tag{29}$$

from which the coefficient $B_{k+1} = \int_0^\pi \psi(\tilde{\theta}_0)\tilde{R}_0 \sin^3\tilde{\theta}_0 P^2_{k+1}(\cos\tilde{\theta}_0)d\tilde{\theta}_0$ are obtained immediately:

$$B_{k+1} = \begin{cases} \frac{b}{\pi\omega a}\cdot\left(\frac{\tilde{R}_0}{a}\right)^{2m-1} & (4m+1), k+1 = 2m, \\ 0, & k+1 = 2m+1. \end{cases} \tag{30}$$

As a result the stresses of screw dislocation in a spheroid are determined from Eqs. (12), (26), (27) and (30). For example, $\sigma_{R\varphi}$ is:

$$\sigma_{R\varphi} = \frac{Gb}{2\pi R}\cot\theta + \frac{Gb}{2\pi R}\sum_{m=1}^{\infty}\frac{(4m+1)}{2m(2m+1)}\left(\frac{R}{a}\right)^{2m}P^1_{2m}(\cos\theta). \tag{31}$$

This solution is identical to those shown by Polonsky et al. (1991a).

4. Elastic fields of segmented inclusion with uniaxial eigenstrain

The use of elastic fields of dislocation loops in the form of Legendre series is convenient for determining the fields of segmented spherical inclusion (SSI), shown in Fig. 4a. Such SSI with uniaxial eigenstrain ε^*_{zz} is modeled by the distribution of prismatic dislocation loops (PLs). These loops are placed on the sphere with radius R_0 from $\theta_0 = \theta_1$ to $\theta_0 = \theta_2$. Then one can easily obtain for example the stresses of SSI with uniaxial eigenstrain ε^*_{zz}, which is constant in magnitude:

$$\sigma^{SSI}_{ij}(R,\theta) = \int_{\theta_1}^{\theta_2}\rho\sigma^{PL}_{ij}(R,\theta,R_0,\theta_0)R_0\sin\theta_0 d\theta_0, \tag{32}$$

where ρ is a density of virtual dislocation loops. In the simplest case the density is constant and related to eigenstrain via $\rho = \frac{\varepsilon^*_{zz}}{b}$, where b is the magnitude of virtual PL Burgers vector.

For example, normal stress component σ^{SSI}_{zz} can be derived from Eq. (32) with the help of Eq. (15a):

$$\sigma^{SSI}_{zz} = \frac{-G\varepsilon^*_{zz}}{2(1-\nu)}\begin{cases} \left(-\sum_{k=1}^{\infty}\left(\frac{R_0}{R}\right)^{k+2}\alpha_k P_{k+1}(\cos\theta) - \sum_{k=1}^{\infty}(k+2)\left(\frac{R_0}{R}\right)^{k+3}\left[\alpha_k\left(\frac{R}{R_0}\right)\cos\theta - \beta_k\right]P_{k+2}(\cos\theta)\right), & R_0 < R \\ \left(-\sum_{k=0}^{\infty}\left(\frac{R}{R_0}\right)^{k}\alpha_{k+1}P_k(\cos\theta) - \sum_{k=0}^{\infty}(k+1)\left(\frac{R}{R_0}\right)^{k}\left[\alpha_{k+2}\left(\frac{R}{R_0}\right)\cos\theta - \beta_{k+2}\right]P_k(\cos\theta)\right), & R < R_0 \end{cases}, \tag{33}$$

where $\alpha_n = \int_{\theta_1}^{\theta_2}\sin^2\theta_0 P^1_n(\cos\theta_0)d\theta_0$, $\beta_n = \int_{\theta_1}^{\theta_2}\cos\theta_0\sin^2\theta_0 P^1_n(\cos\theta_0)d\theta_0$. These last integrals are calculated analytically with the help recurrence relations $\sqrt{1-t^2}P^1_n(t) = \frac{n(n+1)}{2n+1}[P_{n+1}(t) - P_{n-1}(t)]$, $tP_n(t) = \frac{1}{2n+1}[(n+1)P_{n+1}(t) + nP_{n-1}(t)]$ (Bateman and Erdélyi, 1953) and integral formula $\int P_n(t)dt = \frac{1}{2n+1}[P_{n+1}(t) - P_{n-1}(t)]$ (Prudnikov et al., 1983):

$$\alpha_n = \frac{n(n+1)}{(2n+1)}\left[\frac{1}{(2n+3)}(P_{n+2}(t) - P_n(t)) - \frac{1}{2n-1}(P_n(t) - P_{n-2}(t))\right]\Big|_{\cos\theta_2}^{\cos\theta_1}, \tag{34a}$$

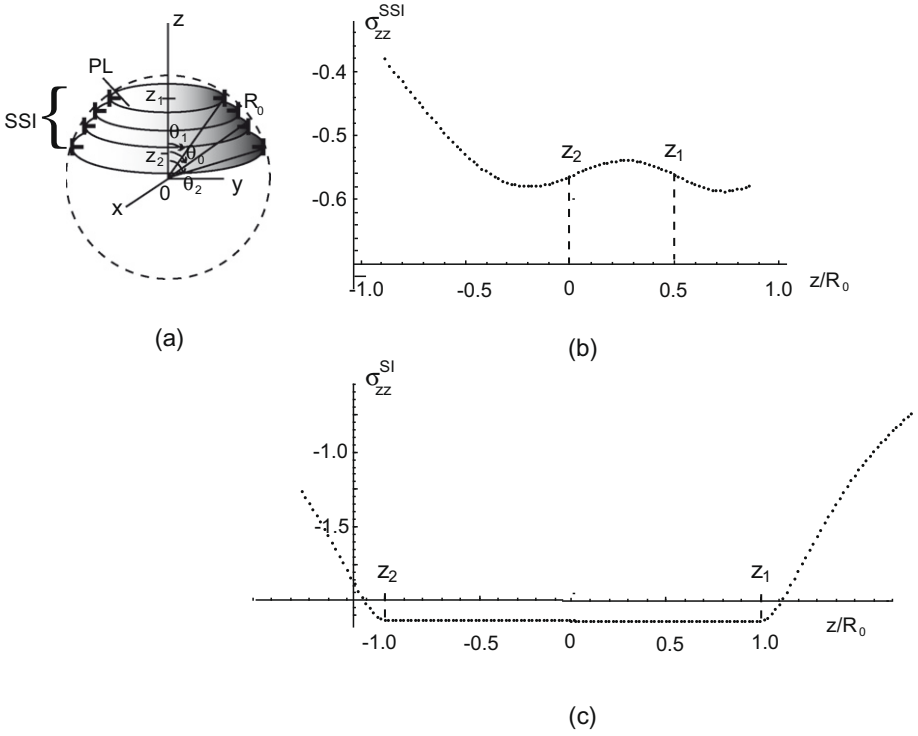

Fig. 4. Segmented spherical inclusion (SSI) with uniaxial eigenstrain ε_{zz}^{*}. (a) Modeling of the inclusion with the help of prismatic dislocation loops (PLs) distributed on a spherical surface from angle θ_1 to angle θ_2; (b) stress component of SSI σ_{zz}^{SSI} along z-axis at $x = 0$, $y = 0$. SSI is characterized by the following parameters: $\theta_1 = \frac{\pi}{3}$, $\theta_2 = \frac{\pi}{2}$; (c) stress component σ_{zz}^{SI} of spherical inclusion SI with uniaxial eigenstrain ε_{zz}^{*} along z-axis ($\theta_1 = 0, \theta_2 = \pi, x = 0, y = 0$). Stresses are in units $\frac{G\varepsilon_{zz}^{*}}{2(1-\nu)}$.

$$\beta_n = \frac{n(n+1)}{(2n+1)}\left[\frac{n+2}{(2n+3)(2n+5)}(P_{n+3}(t) - P_{n+1}(t)) - \frac{1}{(2n-1)(2n+3)}(P_{n+1}(t) - P_{n-1}(t)) - \frac{(n-1)}{(2n-1)(2n-3)}(P_{n-1}(t) - P_{n-3}(t))\right]\Bigg|_{\cos\theta_2}^{\cos\theta_1} \tag{34b}$$

Fig. 4b shows the plot of σ_{zz}^{SSI} stress component of SSI along z-axis for a segmented inclusion bounded by spherical surface of radius R_0 and two planes: $z_1 = R_0 \cos\frac{\pi}{3}$ and $z_2 = R_0 \cos\frac{\pi}{2}$. In general, plot character agrees with the results for the segmented inclusion published by Wu and Du (1999). These authors had shown pick-like peculiarities of the stresses at the vicinity of inclusion plane boundaries. However our calculations demonstrate no pick-like peculiarities. Exploring Eq. (33) with limits$\theta_1 = 0$ and $\theta_2 = \pi$ we plotted in Fig. 4c the stresses for a complete spherical inclusion with uniaxial eigenstrain. These results completely agree with the plots, which can be done on the basis of formulas obtained earlier by Bert et al. (2002), by a different technique.

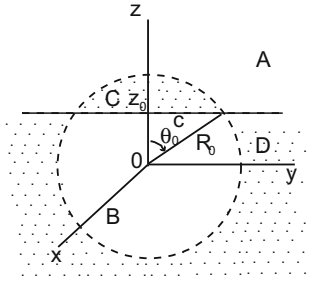

Fig. 5. Regions **A, B, C,** and **D** for the expansion of Lipschitz-Hankel integrals.

5. Summary and conclusions

In the present study the elastic fields of circular twist disclination loops and circular prismatic dislocation loops were found in the form of series with Legendre polynomials, i.e. in terms of spherical harmonics. The representations are based on the expansions of Liphschitz-Hankel integrals (LHIs) with two Bessel functions into Legendre series. The expansions of LHIs were given for two regions defined by a sphere of expansions, i.e. inside and outside the sphere. The radius of the sphere of expansion is determined by defect loop radius and the position of the spherical coordinate origin.

Found representations for elastic fields of circular twist disclination loops were used in the solutions of axisymmetric elasticity boundary-value problems of the theory of defects. New solutions for stresses of a twist disclination loop in a spherical particle and near a spherical pore are given in concise form. The elastic problem for a screw dislocation in a spherical particle is revisited. These solutions were obtained in the framework of general scheme of virtual dislocation–disclination loops.

Spherical harmonics representation for prismatic dislocation loop fields was applied in calculation of elastic fields of segmented spherical inclusions. The easy and straightforward way for calculations of elastic fields of segmented spherical inclusion with uniaxial eigenstrain was demonstrated.

Acknowledgements

The support of Russian Foundation for Basic Research (Project No. 07-01-00659a) and European Commission (Marie Curie Program Project FP7-220419) is gratefully acknowledged.

Appendix A. Expansion of Lipschitz-Hankel integrals with two Bessel function into series with Legendre polynomials

Let us use the following substitution of variables $\gamma = \kappa/c, r = R\sin\ \theta, c = R_0\sin\ \theta_0, z = R\cos\ \theta, z_0 = R_0\cos\ \theta_0$ (see Fig. 1) to transform the LHI with indexes m, n; p, which is given by Eq. (1), to the form:

$$J(m,n;p) = \int_0^\infty J_m(\gamma R_0\sin\theta_0)J_n(\gamma R\sin\theta)e^{-\gamma\mathrm{sgn}(z-z_0)(R\cos\theta - R_0\cos\theta_0)}R_0^{p+1} \times \sin^{p+1}\theta_0\gamma^p d\gamma. \tag{A1}$$

For clarity we assume $\cos\ \theta_0 > 0$ and find the expansion of Eq. (A1) in Legendre polynomials for each of regions A, B, C, and D in spherical coordinates as shown in Fig. 5, separately.

Region A: $R > R_0, (z - z_0) > 0$.

With the designation $\tilde\gamma = \gamma R$ Eq. (A1) becomes:

$$J(m,n;p) = \int_0^\infty J_m\left(\tilde\gamma\frac{R_0}{R}\sin\theta_0\right)J_n(\tilde\gamma\sin\theta)e^{-\tilde\gamma\cos\theta}e^{\tilde\gamma\frac{R_0}{R}\cos\theta_0}\left(\frac{R_0}{R}\right)^{p+1} \times \sin^{p+1}\theta_0\tilde\gamma^p d\tilde\gamma, \tag{A2}$$

With the help of known expansion (Prudnikov et al., 1986):

$$J_m\left(\tilde\gamma\frac{R_0}{R}\sin\theta_0\right)e^{\tilde\gamma\frac{R_0}{R}\cos\theta_0} = (-1)^m\sum_{k=0}^\infty\frac{1}{(k+m)!}\tilde\gamma^k\left(\frac{R_0}{R}\right)^k P_k^m(\cos\theta_0), \tag{A3}$$

where P_k^m are Legendre polynomials ($m = 0$) or associated Legendre polynomials ($m \neq 0$) of the first kind: $P_k^m(t) = (-1)^m(1-t^2)^{\frac{m}{2}}\frac{d^m}{dt^m}P_k(t), m = 1,2,3\ldots$ (Bateman and Erdélyi, 1953), Eq. (A2) can be integrated for each term in the sum (Prudnikov et al., 1983):

$$\begin{aligned}J(m,n;p)_A &= (-1)^m\sin^{p+1}\theta_0\sum_{k=0}^\infty\frac{1}{(k+m)!}\left(\frac{R_0}{R}\right)^{k+p+1}P_k^m(\cos\theta_0)\\ &\times\int_0^\infty J_n(\tilde\gamma\sin\theta)e^{-\tilde\gamma\cos\theta}\tilde\gamma^{k+p}d\tilde\gamma = (-1)^m\sin^{p+1}\theta_0\\ &\times\sum_{k=0}^\infty\frac{\Gamma(k+p+1+n)}{(k+m)!}\left(\frac{R_0}{R}\right)^{k+p+1}\\ &\times P_k^m(\cos\theta_0)P_{k+p}^{-n}(\cos\theta) = (-1)^m\sin^{p+1}\theta_0\\ &\times\sum_{k=0}^\infty\frac{(k+p+n)!}{(k+m)!}\left(\frac{R_0}{R}\right)^{k+p+1}P_k^m(\cos\theta_0)P_{k+p}^{-n}(\cos\theta),\end{aligned} \tag{A4}$$

Here the property $P_k^m = 0$ for $k < m$, $m \geqslant 1$ is used.

Region B: $R < R_0, (z - z_0) < 0$.

In this case the designation $\tilde{\tilde\gamma} = \gamma R_0$ is used to write (A1) as:

$$J(m,n;p) = \int_0^\infty J_m(\tilde{\tilde\gamma}\sin\theta_0)J_n\left(\tilde{\tilde\gamma}\frac{R}{R_0}\sin\theta\right)e^{\tilde{\tilde\gamma}\frac{R}{R_0}\cos\theta}e^{-\tilde{\tilde\gamma}\cos\theta_0} \times \sin^{p+1}\theta_0\tilde{\tilde\gamma}^p d\tilde{\tilde\gamma} \tag{A5}$$

With the help of the known expansion (Prudnikov et al., 1986):

$$J_n\left(\tilde{\tilde\gamma}\frac{R}{R_0}\sin\theta\right)e^{\tilde{\tilde\gamma}\frac{R}{R_0}\cos\theta} = (-1)^n\sum_{k=0}^\infty\frac{1}{(k+n)!}\tilde{\tilde\gamma}^k\left(\frac{R}{R_0}\right)^k P_k^n(\cos\theta). \tag{A6}$$

Eq. (A5) becomes:

$$\begin{aligned}J(m,n;p)_B &= (-1)^n\sin^{p+1}\theta_0\sum_{k=0}^\infty\frac{1}{(k+n)!}\left(\frac{R}{R_0}\right)^k P_k^n(\cos\theta)\\ &\times\int_0^\infty J_n(\tilde{\tilde\gamma}\sin\theta_0)e^{-\tilde{\tilde\gamma}\cos\theta_0}\tilde{\tilde\gamma}^{k+p}d\tilde{\tilde\gamma} = (-1)^n\sin^{p+1}\theta_0\\ &\times\sum_{k=0}^\infty\frac{\Gamma(k+p+1+m)}{(k+n)!}\left(\frac{R}{R_0}\right)^k P_{k+p}^{-m}(\cos\theta_0)P_k^n(\cos\theta)\\ &= (-1)^n\sin^{p+1}\theta_0\sum_{k=0}^\infty\frac{(k+p+m)!}{(k+n)!}\left(\frac{R}{R_0}\right)^k\\ &\times P_{k+p}^{-m}(\cos\theta_0)P_k^n(\cos\theta),\end{aligned} \tag{A7}$$

Region C: $R < R_0, (z - z_0) > 0$.

By analogy with the expansion for region B we write (without proof!):

$$J(m,n;p)_C = (-1)^n\sin^{p+1}\theta_0 \times\sum_{k=0}^\infty\frac{(k+p+m)!}{(k+n)!}\left(\frac{R}{R_0}\right)^k P_{k+p}^{-m}(-\cos\theta_0)P_k^n(-\cos\theta). \tag{A8}$$

Region D: $R > R_0, (z - z_0) < 0$

By analogy with the expansion for region A we write (without proof!):

$$J(m,n;p)_D = (-1)^m\sin^{p+1}\theta_0 \times\sum_{k=0}^\infty\frac{(k+p+n)!}{(k+m)!}\left(\frac{R_0}{R}\right)^{k+p+1}P_k^m(-\cos\theta_0)P_{k+p}^{-n}(-\cos\theta). \tag{A9}$$

We have checked the expansions Eqs. (A4), (A7), (A8) and (A9) numerically for various combination of indexes in LHIs $J(m,n;p)$. We have found that these series give correct results for $\cos\theta_0 < 0$, too. Obtained formulas have the useful properties relating the indexes m, n; p with particular terms in the Legendre expansions: index m in $J(m,n;p)$ enters in Legendre polynomials that depend on the loop position – $P_k^{\pm m}(\pm\cos\theta_0)$, index n enters in Legendre polynomials that depend on the current position $P_k^{\pm n}(\pm\cos\theta)$, index p is included in terms of the type $\sin^{p+1}\theta_0$.

Four expansion with Legendre polynomials Eqs. (A4), (A7), (A8) and (A9) can combined in only two series each of them being valid either for internal region of the sphere of expansion $R < R_0$ or for external region of the sphere of expansion $R > R_0$. We give these results for LHIs $J(m,n;p)$ which are used in displacement and stress fields of a twist disclination loop (TL), see Eqs. (2), (3), and a prismatic dislocation loop (PL), see, Eqs. (4), (5):

$$J(1,0;0)=\begin{cases}-\mathrm{sgn}(z-z_0)\sin\theta_0\sum_{k=1}^{\infty}\frac{1}{(k+1)}\left(\frac{R_0}{R}\right)^{k+1}P_k^1(\cos\theta_0)P_k(\cos\theta), & R_0<R\\ 1+\mathrm{sgn}(z-z_0)\cos\theta_0+\mathrm{sgn}(z-z_0)\sin\theta_0\sum_{k=1}^{\infty}\frac{1}{k}\left(\frac{R}{R_0}\right)^{k}P_k^1(\cos\theta_0)P_k(\cos\theta), & R<R_0\end{cases} \tag{A10a}$$

$$J(1,0;1)=\begin{cases}-\sin^2\theta_0\sum_{k=1}^{\infty}\left(\frac{R_0}{R}\right)^{k+2}P_k^1(\cos\theta_0)P_{k+1}(\cos\theta), & R_0<R\\ -\sin^2\theta_0\sum_{k=0}^{\infty}\left(\frac{R}{R_0}\right)^{k}P_{k+1}^1(\cos\theta_0)P_k(\cos\theta), & R<R_0\end{cases}, \tag{A10b}$$

$$J(1,0;2)=\begin{cases}-\mathrm{sgn}(z-z_0)\sin^3\theta_0\sum_{k=1}^{\infty}(k+2)\left(\frac{R_0}{R}\right)^{k+3}P_k^1(\cos\theta_0)P_{k+2}(\cos\theta), & R_0<R\\ \mathrm{sgn}(z-z_0)\sin^3\theta_0\sum_{k=0}^{\infty}(k+1)\left(\frac{R}{R_0}\right)^{k}P_{k+2}^1(\cos\theta_0)P_k(\cos\theta), & R<R_0\end{cases}, \tag{A10c}$$

$$J(1,1;0)=\begin{cases}\sin\theta_0\sum_{k=1}^{\infty}\frac{1}{k(k+1)}\left(\frac{R_0}{R}\right)^{k+1}P_k^1(\cos\theta_0)P_k^1(\cos\theta), & R_0<R\\ \sin\theta_0\sum\limits_{k=1}^{\infty}\frac{1}{k(k+1)}\left(\frac{R}{R_0}\right)^{k}P_k^1(\cos\theta_0)P_k^1(\cos\theta), & R<R_0\end{cases}, \tag{A10d}$$

$$J(1,1;1)=\begin{cases}\mathrm{sgn}(z-z_0)\sin^2\theta_0\sum_{k=1}^{\infty}\frac{1}{(k+1)}\left(\frac{R_0}{R}\right)^{k+2}P_k^1(\cos\theta_0)P_{k+1}^1(\cos\theta), & R_0<R\\ -\mathrm{sgn}(z-z_0)\sin^2\theta_0\sum_{k=1}^{\infty}\frac{1}{(k+1)}\left(\frac{R}{R_0}\right)^{k}P_{k+1}^1(\cos\theta_0)P_k^1(\cos\theta), & R<R_0\end{cases}, \tag{A10e}$$

$$J(1,1;2)=\begin{cases}\sin^3\theta_0\sum\limits_{k=1}^{\infty}\left(\frac{R_0}{R}\right)^{k+3}P_k^1(\cos\theta_0)P_{k+2}^1(\cos\theta), & R_0<R\\ \sin^3\theta_0\sum_{k=1}^{\infty}\left(\frac{R}{R_0}\right)^{k}P_{k+2}^1(\cos\theta_0)P_k^1(\cos\theta), & R<R_0\end{cases}, \tag{A10f}$$

$$J(2,0;2)=\begin{cases}\sin^3\theta_0\sum_{k=2}^{\infty}\left(\frac{R_0}{R}\right)^{k+3}P_k^2(\cos\theta_0)P_{k+2}(\cos\theta), & R_0<R\\ \sin^3\theta_0\sum_{k=0}^{\infty}\left(\frac{R}{R_0}\right)^{k}P_{k+2}^2(\cos\theta_0)P_k(\cos\theta), & R<R_0\end{cases}, \tag{A10g}$$

$$J(2,1;0)=\begin{cases}-\mathrm{sgn}(z-z_0)\sin\theta_0\sum_{k=2}^{\infty}\frac{1}{k(k+1)(k+2)}\left(\frac{R_0}{R}\right)^{k+1}P_k^2(\cos\theta_0)P_k^1(\cos\theta), & R_0<R\\ \frac{\sin\theta}{\sin\theta_0}\left(\frac{R}{R_0}\right)+\mathrm{sgn}(z-z_0)\left(\cot\theta_0+\frac{1}{4}\sin 2\theta_0\right)\sin\theta\left(\frac{R}{R_0}\right)+ & \\ +\mathrm{sgn}(z-z_0)\sin\theta_0\sum_{k=2}^{\infty}\frac{1}{(k-1)k(k+1)}\left(\frac{R}{R_0}\right)^{k}P_k^2(\cos\theta_0)P_k^1(\cos\theta), & R<R_0\end{cases}, \tag{A10h}$$

$$J(2,1;1)=\begin{cases}-\sin^2\theta_0\sum_{k=2}^{\infty}\frac{1}{(k+1)(k+2)}\left(\frac{R_0}{R}\right)^{k+2}P_k^2(\cos\theta_0)P_{k+1}^1(\cos\theta), & R_0<R\\ -\sin^2\theta_0\sum_{k=1}^{\infty}\frac{1}{k(k+1)}\left(\frac{R}{R_0}\right)^{k}P_{k+1}^2(\cos\theta_0)P_k^1(\cos\theta), & R<R_0\end{cases}, \tag{A10i}$$

$$J(2,1;2)=\begin{cases}-\mathrm{sgn}(z-z_0)\sin^3\theta_0\sum_{k=2}^{\infty}\frac{1}{(k+2)}\left(\frac{R_0}{R}\right)^{k+3}P_k^2(\cos\theta_0)P_{k+2}^1(\cos\theta), & R_0<R\\ \mathrm{sgn}(z-z_0)\sin^3\theta_0\sum_{k=1}^{\infty}\frac{1}{(k+1)}\left(\frac{R}{R_0}\right)^{k}P_{k+2}^2(\cos\theta_0)P_k^1(\cos\theta), & R<R_0\end{cases}, \tag{A10j}$$

$$J(2,2;1)=\begin{cases}\mathrm{sgn}(z-z_0)\sin^2\theta_0\sum_{k=2}^{\infty}\frac{1}{k(k+1)(k+2)}\left(\frac{R_0}{R}\right)^{k+2}P_k^2(\cos\theta_0)P_{k+1}^2(\cos\theta), & R_0<R\\ -\mathrm{sgn}(z-z_0)\sin^2\theta_0\sum_{k=2}^{\infty}\frac{1}{k(k+1)(k+2)}\left(\frac{R}{R_0}\right)^{k}P_{k+1}^2(\cos\theta_0)P_k^2(\cos\theta), & R<R_0\end{cases}, \tag{A10k}$$

To derive Eqs. (A10) we used the following formulas (Bateman and Erdélyi, 1953; Prudnikov et al., 1986): $P_0^{-1}(t)=\sqrt{1-t}/\sqrt{1+t}$, $P_1^{-2}(t)=\frac{(1-t)(2+t)}{6(1+t)}$, $P_k^{-m}(t)=(-1)^m\frac{(k-m)!}{(k+m)!}P_k^m(t)\,(k\geqslant m)$, $P_k^m(-t)=(-1)^{k+m}P_k^m(t)\,(k\geqslant m)$, $P_k^m=0$ at $k<m$, $m\geqslant 1$.

Note that the first term in the in series for $J(1,0;0)$ in the region $R<R_0$ is 1, see Eqs. (A10a). This constant describes the jump that is peculiar to u_z^{Pl}component of PL total displacement. In a similar manner the expansion Eqs. (A10h) of $J(2,1;0)$ in Legendre series in the region $R<R_0$ contains the term $\frac{\sin\theta}{\sin\theta_0}$, which describes the jump in u_φ^{TL}component of TL total displacements. Therefore we can conclude that Legendre series representation explicitly defines the jump in total displacements and allows to separate plastic part out from total displacements.

Appendix B. Analysis of J(1,0;0) at $\theta = 0$

In the following we perform the detailed analysis of the LHI $J(1,0;0)$ at $\theta = 0$. The expansion in this case can be compared with the results reported by Willis et al. (1983).

Integral $J(1,0;0)|_{\theta=0}$ can be presented in terms of elementary functions (Prudnikov et al., 1983):

$$J(1,0;0)|_{\theta=0} = \int_0^\infty J_1(\gamma c)e^{-|z-z_0|\gamma}cd\gamma = 1 - \frac{|z-z_0|}{\sqrt{c^2+(z-z_0)^2}} \tag{B1}$$

From this relation the Legendre series representation follows immediately (see, for example, Arfken, 1985):

$$\begin{aligned} J(1,0;0)|_{\theta=0,z>R_0} &= 1 - \frac{(z-z_0)}{\sqrt{c^2+(z-z_0)^2}} \\ &= 1 - \frac{(z-z_0)}{z}\sum_{k=0}^{\infty}\left(\frac{R_0}{z}\right)^k P_k(\cos\theta_0) \\ &= 1 - \sum_{k=0}^{\infty}\left(\frac{R_0}{z}\right)^k P_k(\cos\theta_0) \\ &\quad + \cos\theta_0\sum_{k=0}^{\infty}\left(\frac{R_0}{z}\right)^{k+1} P_k(\cos\theta_0) \\ &= -\sum_{k=1}^{\infty}\left(\frac{R_0}{z}\right)^k P_k(\cos\theta_0) \\ &\quad + \cos\theta_0\sum_{k=0}^{\infty}\left(\frac{R_0}{z}\right)^{k+1} P_k(\cos\theta_0) \\ &= -\sum_{k=1}^{\infty}\left(\frac{R_0}{z}\right)^k [P_k(\cos\theta_0) \\ &\quad - \cos\theta_0 P_{k-1}(\cos\theta_0)], \end{aligned} \tag{B2a}$$

$$\begin{aligned} J(1,0;0)|_{\theta=0,z<R_0} &= 1 - \frac{|z-z_0|}{\sqrt{c^2+(z-z_0)^2}} \\ &= 1 - \frac{|z-z_0|}{R_0}\sum_{k=0}^{\infty}\left(\frac{z}{R_0}\right)^k P_k(\cos\theta_0) \\ &= 1 - \mathrm{sgn}(z-z_0)\sum_{k=0}^{\infty}\left(\frac{z}{R_0}\right)^{k+1} P_k(\cos\theta_0) \\ &\quad + \mathrm{sgn}(z-z_0)\cos\theta_0\sum_{k=0}^{\infty}\left(\frac{z}{R_0}\right)^k P_k(\cos\theta_0) \\ &= 1 + \mathrm{sgn}(z-z_0)\cos\theta_0 \\ &\quad - \mathrm{sgn}(z-z_0)\sum_{k=0}^{\infty}\left(\frac{z}{R_0}\right)^{k+1} P_k(\cos\theta_0) \\ &\quad + \mathrm{sgn}(z-z_0)\cos\theta_0\sum_{k=1}^{\infty}\left(\frac{z}{R_0}\right)^k P_k(\cos\theta_0) \\ &= 1 + \mathrm{sgn}(z-z_0)\cos\theta_0 - \mathrm{sgn}(z-z_0) \\ &\quad \times\sum_{k=1}^{\infty}\left(\frac{z}{R_0}\right)^k [P_{k-1}(\cos\theta_0) - \cos\theta_0 P_k(\cos\theta_0)], \end{aligned} \tag{B2b}$$

On the other hand from Eq. (A10a) we can write:

$$\begin{aligned} J(1,0;0)|_{\theta=0,R>R_0} &= -\sin\theta_0\sum_{k=1}^{\infty}\frac{1}{(k+1)}\left(\frac{R_0}{R}\right)^{k+1} P_k^1(\cos\theta_0)P_k(1) \\ &= (-1)\sin\theta_0\sum_{k=0}^{\infty}\frac{1}{(k+1)}\left(\frac{R_0}{R}\right)^{k+1} P_k^1(\cos\theta_0) \\ &= -\sum_{k=1}^{\infty}\left(\frac{R_0}{R}\right)^k [P_k(\cos\theta_0) \\ &\quad - \cos\theta_0 P_{k-1}(\cos\theta_0)]; \end{aligned} \tag{B3a}$$

$$\begin{aligned} J(1,0;0)|_{\theta=0,R<R_0} &= 1 + \mathrm{sgn}(z-z_0)\cos\theta_0 + \mathrm{sgn}(z-z_0)\sin\theta_0 \\ &\quad \times\sum_{k=1}^{\infty}\frac{1}{k}\left(\frac{R}{R_0}\right)^k P_k^1(\cos\theta_0)P_k(1) \\ &= 1 + \mathrm{sgn}(z-z_0)\cos\theta_0 - \mathrm{sgn}(z-z_0) \\ &\quad \times\sum_{k=1}^{\infty}\left(\frac{R}{R_0}\right)^k [P_{k-1}(\cos\theta_0) \\ &\quad - \cos\theta_0 P_k(\cos\theta_0)]. \end{aligned} \tag{B3b}$$

Here we have used recurrence relations given by Bateman and Erdélyi (1953):

$$(\nu-\mu+1)P_{\nu+1}^{\mu}(t) - (\nu+\mu+1)tP_{\nu}^{\mu}(t) = \sqrt{1-t^2}P_{\nu}^{\mu+1}(t),$$

$$(\nu-\mu)tP_{\nu}^{\mu}(t) - (\nu+\mu)P_{\nu-1}^{\mu}(t) = \sqrt{1-t^2}P_{\nu}^{\mu+1}(t).$$

It is clear that final results in Eqs. (B2) and (B3) are identical.

It is worthy to note that Eqs. (A8) and (A9), which were given without proof, provide the right results but further analysis is needed.

Formally, at the boundary of expansion, i.e. at $R = R_0$, one can use the series (A4), (A7), (A8) and (A9) with the conditions $J(m,n;p)_A|_{R=R_0} = J(m,n;p)_C|_{R=R_0}, J(m,n;p)_B|_{R=R_0} = J(m,n;p)_D|_{R=R_0}$ to be fulfilled. Numerical calculations do not allow to check this property at the boundary of expansion for arbitrary indexes m, n; p and arbitrary values of the variable θ.

We however are able to demonstrate the property $J(m,n;p)_A|_{R=R_0}, \theta = 0 = J(m,n;p)_C|_{R=R_0,\theta=0}$ on the example of $J(1,0;0)$. Expansions for $J(1,0;0)_A|_{R=R_0,\theta=0}$ and $J(1,0;0)_C|_{R=R_0,\theta=0}$ are found from Eqs. (A10a)

$$\begin{aligned} J(1,0;0)_A|_{R=R_0,\theta=0} &= -\sum_{k=1}^{\infty}[P_k(\cos\theta_0) - \cos\theta_0 P_{k-1}(\cos\theta_0)] \\ &= 1 - \sum_{k=0}^{\infty}P_k(\cos\theta_0) + \sum_{k=0}^{\infty}\cos\theta_0 P_k(\cos\theta_0) \\ &= 1 - \frac{1-\cos\theta_0}{\sqrt{2(1-\cos\theta_0)}}, \end{aligned} \tag{B4a}$$

$$\begin{aligned} J(1,0;0)_C|_{R=R_0,\theta=0} &= 1 + \cos\theta_0 - \sum_{k=1}^{\infty}[P_{k-1}(\cos\theta_0) \\ &\quad - \cos\theta_0 P_k(\cos\theta_0)] \\ &= 1 - \sum_{k=0}^{\infty}P_k(\cos\theta_0) + \sum_{k=0}^{\infty}\cos\theta_0 P_k(\cos\theta_0) \\ &= 1 - \frac{1-\cos\theta_0}{\sqrt{2(1-\cos\theta_0)}}. \end{aligned} \tag{B4b}$$

Here the relationship $\sum_{k=0}^{\infty}P_k(\cos\theta_0) = \frac{1}{\sqrt{2(1-\cos\theta_0)}}$ was used (Prudnikov et al., 1983). Comparison of Eqs. (B4a) and (B4b) proves the equality $J(1,0;0)_A|_{R=R_0,\theta=0} = J(1,0;0)_C|_{R=R_0,\theta=0}$.

References

Aifantis, K.E., Kolesnikova, A.L., Romanov, A.E., 2007. Nucleation of misfit dislocations and plastic deformation in core/shell nanowires. Philosophical Magazine 87, 4731–4757.

Arfken, G., 1985. Mathematical Methods for Physicists, third ed. Academic Press, Inc., San Diego.

Asaro, R.J., 1975. Somigliana dislocations and internal stresses; with application to second phase hardening. International Journal of Engineering Science 13, 271–286.

Bacon, D.J., Groves, P.P., 1970. The dislocation in a semi-infinite isotropic medium. In: Salamon, J.A., de Wit, R., Bullough, R. (Eds.), Fundamental aspects of Dislocation Theory, vol. 1. Nat. Bur. Stand. (US) Spec. Publ., New York, pp. 35–45. No. 317.

Baštecká, J., 1964. Interaction of dislocation loop with free surface. Czechoslovak Journal of Physics B 10, 430–442.
Bateman, H., Erdélyi, A., 1953, second ed. Higher Transcendental Functions, vol. 1 Mc Graw-Hill Book Company, Inc., New York.
Bert, N.A., Kolesnikova, A.L., Romanov, A.E., Chaldyshev, V.V., 2002. Elastic behavior of a spherical inclusion with a given uniaxial dilatation. Physics of the Solid State 44, 2240–2250.
Bondarenko, V.P., Litoshenko, N.V., 1997. Stress–strain state of a spherical layer with circular dislocation loop. International Applied Mechanics 33, 525–531.
Bullough, R., Newman, R.C., 1960. The spacing of prismatic dislocation loops. Philosophical Magazine 5, 921–926.
Bushueva, G.V., Khomyakova, R.D., Predvoditelev, A.A., 1974. Stress field of a circular dislocation loop with an arbitrary Burgers vector. Vestnik Moskovskogo Universiteta. Fizika i Astronomiya. 15, 329–334 (in Russian).
Cai, W., Weinberger, C.R., 2009. Energy of a prismatic dislocation loop in an elastic cylinder. Mathematics and Mechanics of Solids 14, 192–206.
Chou, Y.T., 1963. The energy of circular dislocation loops in thin plates. Acta Metallurgica 11, 829–834.
Chou, T.W., 1971. Twist disclination loops in nonhomogeneous media. Journal of Applied Physics 42, 4092–4094.
Chou, T.-W., Lu, T.-L., 1972. Elastic behaviors of twist disclination loops near free surface. Journal of Applied Physics. 43, 2562–2565.
Chou, T.-W., Lu, T.-L., 1973. Elastic behaviors of wedge disclination loops near a free surface. Materials Science and Engineering 12, 163–166.
Demir, I., Hirth, J.P., Zbib, H.M., 1992a. The Somigliana ring dislocation. Journal of Elasticity 28, 223–246.
Demir, I., Hirth, J.P., Zbib, H.M., 1992b. The extended stress field around a cylindrical crack using the theory of dislocation pile-up. International Journal of Engineering Science 30, 829–845.
Demir, I., Hirth, J.P., Zbib, H.M., 1992c. Remarks on the stress field of the Somigliana dislocation. Mechanics Research Communications 19, 369–374.
Demir, I., Hirth, J.P., Zbib, H.M., 1993. Interaction between two interfacial circular ring dislocations. International Journal of Engineering Science 31, 483–492.
De Wit, R., 1960. Continuum theory of stationary dislocations. In: Seitz, F. (Ed.), Solid State Physics, Advances in Research and Applications, vol. 10. Academic Press, New York. p. 249.
Dundurs, J., Salamon, N.J., 1972. Circular prismatic dislocation loop in a two-phase material. Physica Status Solidi (b) 50, 125–133.
Eason, G., Noble, B., Sneddon, I.N., 1955. On certain integrals of Lipschitz-Hankel type involving products of Bessel functions. Philosophical Transactions of the Royal Soceity of London – Series A 247, 529–551.
Groves, P.P., Bacon, D.J., 1970. The dislocation loop near a free surface. Philosophical Magazine 22, 83–91.
Gryaznov, V.G., Polonsky, I.A., Romanov, E., Trusov, L.I., 1991. Size effects of dislocation stability in nanocrystalls. Physical Review B 44, 42–46.
Hills, D., Kelly, P., Dai, D.N., Korsunsky, A.M., 1996. Solution of Crack Problems (The Distributed Dislocation Technique). Kluwer.
Hirth, J.P., Lothe, J., 1982. Theory of Dislocations, second ed. John Wiley & Sons.
Huang, W., Mura, T., 1970. Elastic fields and energies of a circular edge disclination and a straight screw disclination. Journal of Applied Physics 41, 5175–5179.
Khraishi, T.A., Hirth, J.P., Zbib, H.M., 2000a. The stress field of a general circular Volterra dislocation loops: analytical and numerical approaches. Philosophical Magazine Letters 80, 95–105.
Khraishi, T.A., Hirth, J.P., Zbib, H.M., Khaleel, M.A., 2000b. The displacements and strain–stress fields of a general circular Volterra dislocation loop. International Journal of Engineering Science 38, 251–266.
Kolesnikova, A.L., 2005. Boundary-value problems in theory of defects and their application to nanostructure investigations. Dr. Sci. Thesis. Institute of Problems of Mechanical Engineering, Sankt-Petersburg (in Russian).
Kolesnikova, A.L., Romanov, A.E., 1986. Circular dislocation–disclination loops and their application to boundary problem solution in the theory of defects. Preprint No. 1019, Ioffe Physico-Technical Institute, Leningrad (in Russian).
Kolesnikova, A.L., Romanov, A.E., 1987. Edge dislocation perpendicular to the free surface of a plate. Soviet Technical Physics Letters 13, 272–274.
Kolesnikova, A.L., Romanov, A.E., 2003. Dislocation and disclination loops in the virtual-defect method. Physics of the Solid State 45, 1706–1718.
Kolesnikova, A.L., Romanov, A.E., 2004. Virtual circular dislocation–disclination loop technique in boundary-value problems in the theory of defects. Journal of Applied Mechanics. Transactions of the ASME 71, 409–417.
Korsunsky, A.M., 1996a. The Somigliana ring dislocation revisited. 1. Papkovich potential solutions for dislocations in an infinite space. Journal of Elasticity 44, 97–114.
Korsunsky, A.M., 1996b. The Somigliana ring dislocation revisited. 2. Solutions for dislocations in a half-space and in one of two perfectly bonded dissimilar half-space. Journal of Elasticity 44, 115–129.
Kröner, E., 1958. Kontinuumstheotie der Versetzungen und Eigenspannung. Springer, Berlin.
Kroupa, F., 1960. Circular edge dislocation loop. Czechoslovak Journal of Physics B 10, 284–293.
Kroupa, F., 1962. Interaction between prismatic dislocation loops and straight dislocations. Part I. Philosophical Magazine 7, 783–801.
Kuo, H.H., Mura, T., 1972a. Elastic field and strain energy of circular wedge disclination. Journal of Applied Physics 43 (4), 1454–1457.
Kuo, H.H., Mura, T., 1972b. Circular disclinations and interface effects. Journal of Applied Physics 43, 3936–3942.
Kuo, H.H., Mura, T., Dundurs, J., 1973. Moving circular twist disclination loop in homogeneous and two-phase materials. International Journal of Engineering Science 11, 193–201.
Li, J.C.M., Gilman, J.J., 1970. Disclination loops in polymers. Journal of Applied Physics 41, 4248–4256.
Liu, G.C.T., Li, J.C.M., 1971. Strain energy of disclination loops. Journal of Applied Physics 42, 3313–3315.
Love, A.E.H., 2003. A Treatise on the Mathematical Theory of Elasticity, fourth ed. Dover.
Lurie, A.I., 1970. Theory of Elasticity. Nauka, Moscow (in Russian).
Marcikowski, M.J., Sree Harsha, K.S., 1968. Properties of finite circular dislocation glide loops. Journal of Applied Physics 39, 1775–1783.
Mura, T., 1987. Micromechanics of Defects in Solids, second ed. Martinus Nijhoff Publishers, The Netherland.
Ovidko, I.A., Sheinerman, A.G., 2004. Misfit dislocation loops in composite nanowires. Philosophical Magazine 84, 2103–2118.
Owen, D.R.J., Mura, T., 1967. Dislocation configurations in cylindrical coordinates. Journal of Applied Physics 38, 2818–2825.
Paynter, R.J.H., Hills, D.A., 2009. The effect of path cut on Somigliana ring dislocations in a half-space. International Journal of Solids and Structures 46, 412–432.
Paynter, R.J.H., Hills, D.A., Korsunsky, A.M., 2007. The effect of path cut on Somigliana ring dislocations elastic fields. International Journal of Solids and Structures 44, 6653–6677.
Polonsky, I.A., Romanov, A.E., Gryaznov, V.G., Kaprelov, A.M., 1991a. Screw dislocation in an elastic sphere. Czechoslovak Journal of Physics 41, 1249–1255.
Polonsky, I.A., Romanov, A.E., Gryaznov, V.G., Kaprelov, A.M., 1991b. Disclination in an elastic sphere. Philosophical Magazine A 64, 281–287.
Povstenko, Y.Z., 1995. Circular dislocation loops in non-local elasticity. Journal of Physics D: Applied Physics 28, 105–111.
Povstenko, Y.Z., Matkovski, O.A., 2000. Circular disclination loops in nonlocal elasticity. International Journal of Solids and Structures 37, 6419–6432.
Prudnikov, A.P., Brychkov, Yu.A., Marichev, O.I., 1983. Integrals and Series. Special functions. Nauka, Moscow (in Russian).
Prudnikov, A.P., Brychkov, Yu.A., Marichev, O.I., 1986. Integrals and Series. Additional Chapters. Nauka, Moscow (in Russian).
Romanov, A.E., Vladimirov, V.I., 1992. Disclinations in Crystalline Solids. In: Nabarro, F.N.R. (Ed.), Dislocations in Solids 9. North Holland, Amsterdam, pp. 191–402.
Sackfield, A., Barber, J.R., Hills, D.A., Truman, C.E., 2002. A shrink-fit subject to torsion. European Journal of Mechanics 21, 73–84.
Salamon, N.J., 1981. The circular glide dislocation loop lying in an interface. Journal of Mechanics and Physics of Solids 29, 1–11.
Salamon, N.J., Dundurs, J., 1971. Elastic fields of a dislocation loop in a two-phase material. Journal of Elasticity 1, 153–164.
Salamon, N.J., Dundurs, J., 1977. A circular glide dislocation loop in a two-phase material. Journal of Physics C: Solid State Physics 10, 497–507.
Salamon, N.J., Walter, G.G., 1979. Limits of Lipschitz-Hankel Integrals. Journal of Institute of Mathematical Applications 24, 237–254.
Steketee, J., 1958. On Volterra's dislocations in a semi-infinite elastic medium. Canadian Journal of Physics 36, 192–205.
Tikhonov, L.V., 1967. About behavior of dislocation loops in thick plate, which have free surfaces under time periodic temperature variation. Fizika Metallov and Metallovedenie 24, 577–587 (in Russian).
Vagera, I., 1970a. Long range elastic interaction of prismatic dislocation loop with grain boundary. Czechoslovak Journal of Physics B 20 (6), 702–710.
Vagera, I., 1970b. Long range force on dislocation loop doe to grain boundary. Czechoslovak Journal of Physics B 20 (12), 1278–1284.
Was, G.S., 2007. Fundamentals of Radiation Materials Science: Metals and Alloys. Springer.
Watson, G.N., 1944. The Theory of Bessel Functions, second ed. Cambridge University Press.
Willis, J.R., Bullough, B., Stoneham, A.M., 1983. The effect of dislocation loop on the lattice parameter, determined by X-ray diffraction. Philosophical Magazine A 48, 95–107.
Wu, L.Z., Du, S.Y., 1999. The elastic field with a hemispherical inclusion. Proceedings of the Royal Society of London A 455, 879–891.